CGT: Consistency Guided Training in Semi-Supervised Learning

Nesreen Hasan*, Farzin Ghorban*, Jörg Velten and Anton Kummert
Faculty of Electrical, Information and Media Engineering, University of Wuppertal, Germany

Keywords: Semi-Supervised Learning, Consistency Regularization, Data Augmentation.

Abstract: We propose a framework, CGT, for semi-supervised learning (SSL) that involves a unification of multiple image-based augmentation techniques. More specifically, we utilize Mixup and CutMix in addition to introducing one-sided stochastically augmented versions of those operators. Moreover, we introduce a generalization of the Mixup operator that regularizes a larger region of the input space. The objective of CGT is expressed as a linear combination of multiple constituents, each corresponding to the contribution of a different augmentation technique. CGT achieves state-of-the-art performance on the SVHN, CIFAR-10, and CIFAR-100 benchmark datasets and demonstrates that it is beneficial to heavily augment unlabeled training data.

1 INTRODUCTION

Obtaining a fully labeled dataset for training deep models is known to be expensive and time-consuming. SSL aims to leverage a large amount of unlabeled data along with a small number of labeled data to improve the model performance. In recent years, various SSL approaches have been developed and have shown remarkable results on different benchmark datasets (Tarvainen and Valpola, 2017; Luo et al., 2018; Ke et al., 2019; Qiao et al., 2018; Verma et al., 2019b; Ghorban et al., 2021; Li et al., 2019; Xie et al., 2019).

Perturbation-based methods, a dominant approach in SSL, are inspired by the *smoothness assumption* which states that points from high-density regions in the data manifold that are close to each other are likely to share the same label. These approaches require consistency of predictions under different perturbations. The perturbations used in recent works can be categorized into *image-* and *model-based* perturbations. In the first case, perturbations are applied to input samples whereas in the second case the hidden layers in the model induce perturbation, i.e., two evaluations of the same input yield different results.

The procedure we propose in this work relies on unifying multiple advanced data augmentation methods that have shown to work well. In our framework, we utilize Mixup (Zhang et al., 2018) and Cutmix (Yun et al., 2019) operators besides introducing augmented versions of those operators in addition to a generalization of the Mixup operator. These augmented versions apply a set of common augmentation transformations stochastically on one of the inputs to those operators. The objective of our framework is a linear combination of multiple constituents, each belonging to a different augmentation transformation.

The remainder of this work is organized as follows. In Sec. 2, we review relevant and related consistency-based and augmentation approaches. Section 3 briefly introduces and discusses the image augmentation operations that we use for developing our approach which we introduce in Sec. 4. Finally, in Sec. 5, we present and discuss our results on three different datasets and give a conclusion in Sec. 6.

2 RELATED WORK

In this section, we briefly discuss works in SSL that are closely related to ours. We focus on works that conceptually follow the approach of enforcing consistency on unlabeled data points, i.e., penalize inconsistent predictions of a data point under different transformations. Furthermore, we review recently proposed augmentation methods.

In Π-model (Laine and Aila, 2016), each sample undergoes two different perturbations that are assumed to not change the data identity. For each pair of perturbed data points, any inconsistency in predictions is penalized. TE (Laine and Aila, 2016) fol-

* Authors contributed equally.

Hasan, N., Ghorban, F., Velten, J. and Kummert, A.
CGT: Consistency Guided Training in Semi-Supervised Learning.
DOI: 10.5220/0010771700003124
In *Proceedings of the 17th International Joint Conference on Computer Vision, Imaging and Computer Graphics Theory and Applications (VISIGRAPP 2022) - Volume 5: VISAPP*, pages 55-64
ISBN: 978-989-758-555-5; ISSN: 2184-4321

lows the same concept with the difference that the targets are constructed via exponential moving average (EMA) of previous model predictions. In MT (Tarvainen and Valpola, 2017), targets are generated by an EMA model constructed via EMA of previous model weights. The aforementioned consistency regularization methods consider only perturbations around single data points. SNTG (Luo et al., 2018) considers the connections between all data points and regularizes the neighboring points on a learned teacher graph.

Recently, interpolation-based regularization methods (Zhang et al., 2018; Tokozume et al., 2018; Verma et al., 2019a) have been proposed for supervised learning, achieving state-of-the-art performances across a variety of tasks. This regularization scheme requires the use of the Mixup operator (Zhang et al., 2018). Similar to data augmentation, Mixup is a way of artificially expanding the volume of a training set and thus increasing data diversity. Mixup creates new training samples by linearly combining two samples and their corresponding labels. The regularization of interpolating between distant data points via Mixup affects large regions of the input space. Thus, this regularization scheme became successfully adopted in SSL (Verma et al., 2019b; Ma et al., 2020; Berthelot et al., 2019; Nair et al., 2019; Berthelot et al., 2020).

In ICT (Verma et al., 2019b), authors apply Mixup on labeled and unlabeled data points by replacing the missing labels with predictions of an EMA model and show impressive improvement over previous methods. AdvMixup (Ma et al., 2020) applies Mixup regularization on real and adversarial samples (Goodfellow et al., 2015; Miyato et al., 2018). MixMatch (Berthelot et al., 2019) and RealMix (Nair et al., 2019) present holistic approaches that combine various dominant SSL approaches with Mixup. More concretely, to name some, (Berthelot et al., 2019) uses sharpening and label average over multiple augmentations and interpolates samples between labeled and unlabeled data points. PLCB (Arazo et al., 2020) proposes the use of pseudo-labeling and demonstrates that enforcing interpolation consistency helps to prevent an overfit to incorrect pseudo-labels. ReMixMatch (Berthelot et al., 2020) is the direct descendant of MixMatch and extends its holistic approach by the concepts of distribution alignment and augmentation anchoring. Augmentation anchoring differs from the label average over multiple augmentations in the aspect that it requires predictions of strong augmentations of a sample to be close to the prediction of a weakly augmented version of that sample. Moreover, the authors use an extended set of augmentations that originates from AutoAugment (Cubuk et al., 2018).

Common data augmentations have recently gained attention in various vision domains (Ghorban et al., 2018; Zhong et al., 2020; Ghiasi et al., 2018; Hendrycks* et al., 2020; Cubuk et al., 2018; Cubuk et al., 2020) and have shown to be an important component in SSL. These augmentations can dramatically change the pixel content of a sample. AutoAugment (Cubuk et al., 2018) learns optimal augmentation strategies from data using reinforcement learning to choose a sequence of operations as well as their probability of application and magnitude. Authors in (Lim et al., 2019; Ho et al., 2019) optimize the AutoAugment algorithm to find more efficient policies. RandAugment (Cubuk et al., 2020) is a simplification of AutoAugment with a significantly reduced hyperparameter search space.

3 PRELIMINARIES

Consider a training set that consists of N samples, out of which L have labels and the others are unlabeled. Let $\mathcal{L} = \{(x_i, y_i)\}_{i=1}^{L}$ be the labeled set and $\mathcal{U} = \{x_i\}_{i=L+1}^{N}$ be the unlabeled set with $y_i \in \{0,1\}^K$ being one-hot encoded labels and K the number of classes. Considering consistency regularization in SSL, the objective is to minimize the following generic loss

$$\mathscr{L} = \mathscr{L}_S + w\,\mathscr{L}_C, \tag{1}$$

where $\mathscr{L}_S$ is the cross-entropy supervised learning loss over $\mathcal{L}$, and $\mathscr{L}_C$ is the consistency regularization term weighted by w. $\mathscr{L}_C$ penalizes inconsistent predictions of unlabeled data.

3.1 Augmentation Techniques

There exist a variety of augmentation techniques and recent literature has demonstrated their success in supervised learning (DeVries and Taylor, 2017; Zhang et al., 2018; Yun et al., 2019; Hendrycks* et al., 2020; Ghiasi et al., 2018; Zhong et al., 2020). In this section, we briefly discuss four of these techniques from which three are key contributors to our approach.

Let $x_i \in \mathbb{R}^{W\times H\times C}$ and y_i denote a training image and its one-hot encoded label, respectively. Let (x_1, y_1) and (x_2, y_2) denote two given pairs of samples and their labels.

Mixup. Mixup (Zhang et al., 2018) is able to create an infinite set of new pairs using a linear combination defined via the following operator

$$\Big(\mathrm{Mixup}_\lambda(x_1,x_2) = \lambda x_1 + (1-\lambda)x_2, \quad \mathrm{Mixup}_\lambda(y_1,y_2) = \lambda y_1 + (1-\lambda)y_2\Big), \tag{2}$$

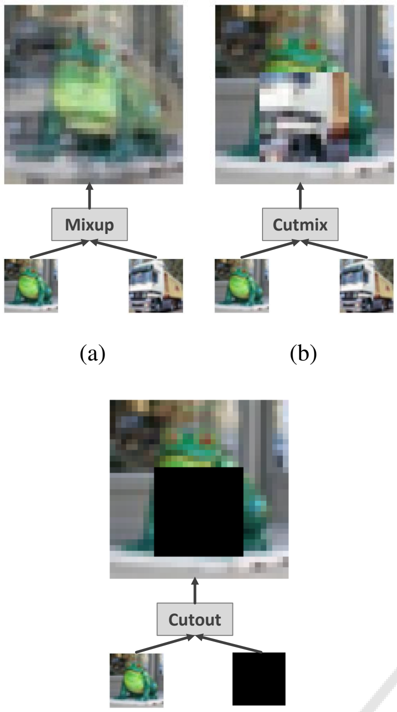

(a) (b)

(c)

Figure 1: Visualizations of inputs and outputs of Mixup (a), Cutmix (b), and Cutout (c) augmentation techniques.

where λ is a randomly sampled parameter from the distribution $\mathrm{Beta}(\beta,\beta)$ with β being a hyperparameter.
Cutmix. Cutmix (Yun et al., 2019) relies on generating new pairs from two input pairs where a rectangular part of x_1 is replaced by a rectangular part of the same size cropped from x_2. It is defined as

$$\Big(\mathrm{Cutmix}_\lambda(x_1,x_2) = M_\lambda \odot x_1 + (I - M_\lambda) \odot x_2,$$
$$\mathrm{Mixup}_\lambda(y_1,y_2) = \lambda y_1 + (1-\lambda) y_2\Big), \qquad (3)$$

where $M_\lambda \in \{0,1\}^{W\times H}$ is a binary mask filled with ones for the cropping region and zeros otherwise. I is a binary mask filled with ones, and $\odot$ is the elementwise multiplication operator. The rectangle coordinates defined as (r_x, r_y, r_w, r_h) are uniformly sampled as

$$r_x \sim U(0,W),\, W\sqrt{1-\lambda} = r_w \sim U(0,w),$$
$$r_y \sim U(0,H),\, H\sqrt{1-\lambda} = r_h \sim U(0,h), \qquad (4)$$

with λ being sampled from $\mathrm{Beta}(\beta,\beta)$ and corrected so that the cropped area ratio becomes $\frac{r_w \times r_h}{W \times H} = 1 - \lambda$. w and h denote hyperparameters.
Cutout. Cutout (DeVries and Taylor, 2017) can be considered as a special case of Cutmix and can be applied using Eq. 3 with x_2 being replaced by a zero matrix of the same dimension. However, in contrast to Cutmix and Mixup, Cutout does not apply any operation on the targets.

Visualizations of the inputs and outputs of the Mixup with $\lambda = 0.4$, Cutmix with $1-\lambda = 0.25$, i.e., $r_w = r_h = 16$, and Cutout operations are shown in Fig. 1.
RandAugment. RandAugment (Cubuk et al., 2020) uses a set of 14 traditional augmentation transformations. Essentially, it uses two parameters, N and M, where N is the number of augmentation transformations to apply sequentially on an image and M is the magnitude of the different transformations.

3.2 Consistency Regularization

Augmentation methods discussed in Sec. 3.1 were initially introduced in the context of supervised learning for enhancing the generalization capability of deep models. Recently, ICT (Verma et al., 2019b) has adapted interpolation consistency to semi-supervised learning by using guessed labels of an EMA model. The consistency term for unlabeled data becomes

$$\mathcal{L}_C = \mathbb{E}_{x_i,x_j \in \mathcal{U}}\, \mathbb{E}_{\lambda\sim\mathrm{Beta}(\beta,\beta)}$$
$$l\Big(C_\theta(\mathrm{Mixup}_\lambda(x_i,x_j)), \mathrm{Mixup}_\lambda(C_{\theta'}(x_i), C_{\theta'}(x_j))\Big), \qquad (5)$$

where C_θ and $C_{\theta'}$ refer to the classifier and EMA models parameterized by θ and θ', respectively, and l is a measure of distance. For the supervised part, a similar objective applies to the labeled data

$$\mathcal{L}_S = \mathbb{E}_{(x_i,y_i),(x_j,y_j)\in\mathcal{L}}\, \mathbb{E}_{\lambda\sim\mathrm{Beta}(\beta,\beta)}$$
$$l\Big(C_\theta(\mathrm{Mixup}_\lambda(x_i,x_j)), \mathrm{Mixup}_\lambda(y_i,y_j)\Big). \qquad (6)$$

We reproduce ICT without changing any setting using Tensorflow (Abadi et al., 2016). However, for our baseline which is practically a duplicate of ICT, we apply two changes. First, we omit the ZCA transformation of the input data and only normalize the samples to lie in the range $[0,1]$. Second, we rectify a discrepancy in the target calculation in Eq. 5, i.e., while authors apply Mixup on the logits of $C_{\theta'}$ to feed the softmax function and calculate the targets, we apply Mixup directly on the softmax outputs. We notice that these changes lead to a slight improvement in performance.

Table 1 compares ICT to our adaptation of it, ICT*. Moreover, since our framework allows the replacement of the Mixup operator through any in Sec. 3.1 discussed augmentation methods, Tab. 1 shows a comparison between the three related methods Mixup, Cutmix, and Cutout on CIFAR-10 test set using 4000 labeled samples, see Sec. 5.1. For Cutmix and Cutout, we use $w \times h = 16 \times 16$ cropped area

Table 1: Comparison between test error rates [%] of ICT and our implementation of it (ICT*) on CIFAR-10 using 4000 labels. Errors for Cutmix, Cutout, and the two linear combinations (shown at the last two coloums) are obtained by adapting them into ICT* while replacing Mixup. Results are averaged over three runs using the CNN-13 architecture (Laine and Aila, 2016).

CIFAR-10, $L = 4000$					
ICT	Mixup (ICT*)	Cutmix	Cutout	Mixup&Cutmix	Mixup&Cutmix&Cutout
7.39 ± 0.11	6.90 ± 0.16	6.73 ± 0.20	8.22 ± 0.09	$\mathbf{6.23 \pm 0.01}$	6.53 ± 0.06

size as suggested by the authors in (Yun et al., 2019; DeVries and Taylor, 2017).

We observe that Cutmix and Mixup achieve comparable performances and significantly outperform Cutout. As discussed before, Cutout can be considered as a special case of Cutmix, however, while Cutmix crops a region of an image and proportionally adjusts the targets of the remaining patch, Cutout omits this target adjustment. In (Yun et al., 2019), authors are able to enhance the performance of Cutout by combining it with label smoothing. Therefore, we think that label smoothing may also help in our setting. Furthermore, we observe that the two straightforward combinations, i.e., linear combinations of the corresponding objectives, shown in the last two columns, not only outperform all three basic augmentation methods but Mixup&Cutmix also outperforms more advanced and recent methods such as (Berthelot et al., 2019; Nair et al., 2019; Ma et al., 2020), see Tab. 2. This observation together with the simplicity of those augmentation techniques motivated us to further explore and develop this framework.

4 CGT FRAMEWORK

Our framework unifies several of the previously mentioned augmentation techniques, namely Mixup, Cutmix, RandAugment, and 3-Mixup which we describe in detail in the following section. For applying the augmentations on unlabeled data, as for ICT, we rely on guessed labels obtained using an EMA model, $C_{\theta'}$. Moreover, we propose a procedure that slightly improves the performance of ICT and its derivatives, mentioned in the previous section, in the final stage of the training.

4.1 Augmentation Operators

In this section, we introduce our augmented Mixup and Cutmix operators in addition to the 3-Mixup operator which is an extension of the Mixup operator and regularizes a larger region of the input space.

Let $\mathcal{B} = \{(x_i, y_i)\}_{i=1}^{B} \equiv (\mathcal{X}, \mathcal{Y})$ be a batch of B samples, $\mathcal{X}$, and their corresponding true or guessed labels depending on whether $x_i \in \mathcal{L}$ or $x_i \in \mathcal{U}$. We denote two random permutations of $(\mathcal{X}, \mathcal{Y})$ as $(\mathcal{X}, \mathcal{Y})'$ and $(\mathcal{X}, \mathcal{Y})''$ and in order to distinguish between them elementwise, we use the following notation

$$
\begin{aligned}
(\mathcal{X}, \mathcal{Y})' &\equiv (\mathcal{X}', \mathcal{Y}') &&\equiv \{(x_i', y_i')\}_{i=1}^{B}, \\
(\mathcal{X}, \mathcal{Y})'' &\equiv (\mathcal{X}'', \mathcal{Y}'') &&\equiv \{(x_i'', y_i'')\}_{i=1}^{B}.
\end{aligned} \tag{7}
$$

Accordingly, the following refers to the operators applied on the samples of a batch

$$
\begin{aligned}
\mathrm{Mixup}_\lambda(\mathcal{X}, \mathcal{X}') &\equiv \{\mathrm{Mixup}_\lambda(x_i, x_i')\}_{i=1}^{B}, \\
\mathrm{Cutmix}_\lambda(\mathcal{X}, \mathcal{X}') &\equiv \{\mathrm{Cutmix}_\lambda(x_i, x_i')\}_{i=1}^{B}.
\end{aligned} \tag{8}
$$

We define the following augmented Mixup and Cutmix operators as

$$
\mathrm{Mixup}_\lambda^{\zeta}(\mathcal{X}, \mathcal{X}') \equiv \{\mathrm{Mixup}_\lambda(x_i, \zeta(x_i'))\}_{i=1}^{B}, \tag{9}
$$

$$
\mathrm{Cutmix}_\lambda^{\zeta}(\mathcal{X}, \mathcal{X}') \equiv \{\mathrm{Cutmix}_\lambda(x_i, \zeta(x_i'))\}_{i=1}^{B}. \tag{10}
$$

Algorithm 1: Consistency Guided Training (CGT) Algorithm.

Input:
N_{epoch}, N_{batch}: #epochs, #batches
B: batch size
$\mathcal{L}$, $\mathcal{U}$: labeled and unlabeled sets
C_θ, $C_{\theta'}$: models with parameters θ and θ'
$\boldsymbol{\lambda_S}, \boldsymbol{\lambda_C}$: supervised and consistency weights
$w(t) \in [0, w_{\max}]$: ramp-up function
τ: starting epoch for overwriting θ
β: coefficient for Beta distribution
α: rate of EMA
for $e = 1, \ldots, N_{\text{epoch}}$ **do**
  for $b = 1, \ldots, N_{\text{batch}}$ **do**
    $\mathcal{B}_l \leftarrow \{(x_i, y_i)\}_{i=1}^{B}$, $(x_i, y_i) \in \mathcal{L}$
    $\mathcal{B}_u \leftarrow \{(x_i, C_{\theta'}(x_i))\}_{i=1}^{B}$, $x_i \in \mathcal{U}$
    $\lambda, \boldsymbol{\lambda} = (\lambda_i)_{i=1}^{3}$, $\lambda, \lambda_i \sim \mathrm{Beta}(\beta, \beta)$
    $L_S \leftarrow l_S(\mathcal{B}_l, \theta, \lambda, \boldsymbol{\lambda_S})$ ▷ Eq. 15
    $L_C \leftarrow l_C(\mathcal{B}_u, \theta, \lambda, \boldsymbol{\lambda}, \boldsymbol{\lambda_C})$ ▷ Eq. 18
    $t \leftarrow e + b/N_{\text{batch}}$
    $\theta \leftarrow \mathrm{SGD}(\theta, L_S + w(t) L_C)$
    $\theta' \leftarrow \alpha\theta' + (1-\alpha)\theta$ ▷ apply EMA
  end
  if $e \geq \tau$ **then**
    $\theta \leftarrow \theta'$ ▷ overwrite θ
  end
end
return θ'

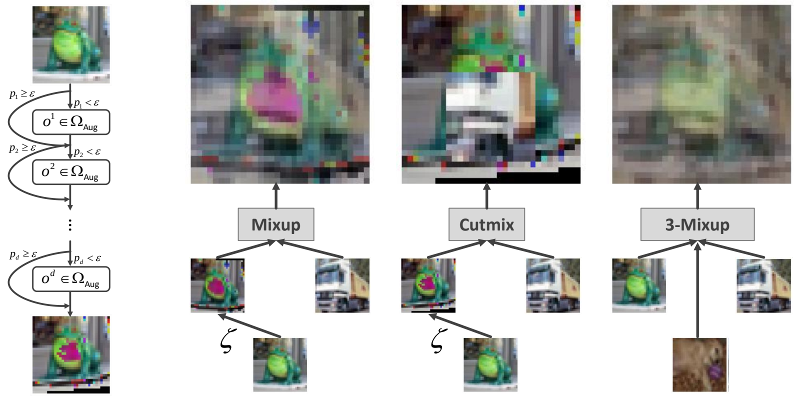

(a) (b) (c) (d)

Figure 2: (a) illustrates the composite function, ζ, that applies a series of augmentation transformations stochastically with a maximum length of d. (b) and (c) visualize our augmented Mixup and Cutmix operations, respectively. (d) visualizes the 3-Mixup operation.

The function ζ, illustrated in Fig. 2 (a), is a composite function that applies a series of augmentation transformations stochastically and has a maximum length of d,

$$\zeta(x, p_1, p_2, \cdots, p_d) = o^d_{p_d}\left(\cdots o^2_{p_2}\left(o^1_{p_1}(x)\right)\cdots\right), \tag{11}$$

where

$$o^i_{p_i}(x) = \begin{cases} o^i(x) & \text{if } p_i < \varepsilon \\ x & \text{otherwise,} \end{cases} \tag{12}$$

with o^i being randomly chosen from Ω_{Aug}. Ω_{Aug} is a set of traditional augmentation transformations, ε is a hyperparameter, and p_i is sampled from a uniform distribution $U(0,1)$. In Eqs. 9 and 10, we drop the parameters of ζ for brevity. Derived from the Mixup operator, we introduce a new operator that we name *3-Mixup* and define as

$$\text{3-Mixup}_{\boldsymbol{\lambda}}(\mathcal{X}, \mathcal{X}', \mathcal{X}'') \equiv \{\text{3-Mixup}_{\boldsymbol{\lambda}}(x_i, x'_i, x''_i)\}_{i=1}^{B}, \tag{13}$$

where new data pairs are created according to

$$\Big(\text{3-Mixup}_{\boldsymbol{\lambda}}(x_1, x_2, x_3) = \sum_{i=1}^{3} \lambda_i x_i,$$
$$\text{3-Mixup}_{\boldsymbol{\lambda}}(y_1, y_2, y_3) = \sum_{i=1}^{3} \lambda_i y_i\Big), \tag{14}$$

with $\boldsymbol{\lambda} = (\lambda_i)_{i=1}^3$ and λ_i being randomly sampled parameters from the distribution $\text{Beta}(\beta, \beta)$ under the condition $\sum_{i=1}^{3} \lambda_i = 1$. The aforementioned operators are visualized in Fig. 2.

4.2 Training Objectives

Our training routine unifies the augmentation operators mentioned in Sec. 4.1. The supervised loss is given by

$$l_S(\mathcal{B}, \theta, \lambda, \boldsymbol{\lambda_S}) = \sum_{i=1}^{2} \lambda_S^i \, l_S^i(\mathcal{B}, \theta, \lambda), \text{ with} \tag{15}$$

$$l_S^1(\mathcal{B}, \theta, \lambda) = \text{CE}\Big(C_\theta\big(\text{Mixup}_\lambda(\mathcal{X}, \mathcal{X}')\big), \text{Mixup}_\lambda(\mathcal{Y}, \mathcal{Y}')\Big), \tag{16}$$

$$l_S^2(\mathcal{B}, \theta, \lambda) = \text{CE}\Big(C_\theta\big(\text{Cutmix}_\lambda(\mathcal{X}, \mathcal{X}')\big), \text{Mixup}_\lambda(\mathcal{Y}, \mathcal{Y}')\Big), \tag{17}$$

where CE stands for the categorical cross-entropy function. Our consistency loss consists of three contributors,

$$l_C(\mathcal{B}, \theta, \lambda, \boldsymbol{\lambda}, \boldsymbol{\lambda_C}) = \sum_{i=1}^{2} \lambda_C^i \, l_C^i(\mathcal{B}, \theta, \lambda) + \lambda_C^3 \, l_C^3(\mathcal{B}, \theta, \boldsymbol{\lambda}), \tag{18}$$

where $l_C^{1,2}$ are similar to $l_S^{1,2}$ except for three changes: (a) we replace CE function with L2 function, (b) $\mathcal{Y}$ are guessed labels obtained using $C_{\theta'}(\mathcal{X})$, and (c) $\text{Mixup}_\lambda(\mathcal{X}, \mathcal{X}')$ and $\text{Cutmix}_\lambda(\mathcal{X}, \mathcal{X}')$ are replaced with $\text{Mixup}_\lambda^\zeta(\mathcal{X}, \mathcal{X}')$ and $\text{Cutmix}_\lambda^\zeta(\mathcal{X}, \mathcal{X}')$, respectively. In addition, we define

$$l_C^3(\mathcal{B}, \theta, \boldsymbol{\lambda}) = \text{L2}\Big(C_\theta\big(\text{3-Mixup}_{\boldsymbol{\lambda}}(\mathcal{X}, \mathcal{X}', \mathcal{X}'')\big), \text{3-Mixup}_{\boldsymbol{\lambda}}(\mathcal{Y}, \mathcal{Y}', \mathcal{Y}'')\Big).$$

The total loss is then calculated via Eq. 1 with

$$\begin{aligned} \mathcal{L}_S &= \mathbb{E}_{\mathcal{B} \in \mathcal{L}, \lambda} \, l_S(\mathcal{B}, \theta, \lambda, \boldsymbol{\lambda_S}), \\ \mathcal{L}_C &= \mathbb{E}_{\mathcal{B} \in \mathcal{U}, \lambda, \boldsymbol{\lambda}} \, l_C(\mathcal{B}, \theta, \lambda, \boldsymbol{\lambda}, \boldsymbol{\lambda_C}). \end{aligned} \tag{19}$$

There exists a mutual influence between C_θ and $C_{\theta'}$. In the early stages of the training, C_θ improves rapidly and causes a slower improvement of $C_{\theta'}$ through EMA. However, after further training $C_{\theta'}$ improves over C_θ and since $C_{\theta'}$ functions as a target generator, an improvement of $C_{\theta'}$ leads to an improvement of C_θ. Both models, however, reach eventually plateaus. At that stage of the training, we notice that, using our setting, overwriting θ with θ' periodically starting from epoch τ leads to further improvement in C_θ and consequently to an improvement in $C_{\theta'}$. Algorithm 1 summarizes the CGT training.

5 EXPERIMENTS

5.1 Datasets

We follow the common practice in evaluating SSL approaches (Verma et al., 2019b; Kuo et al., 2020; Tarvainen and Valpola, 2017; Wu et al., 2019; Kamnitsas et al., 2018) and report the performance of our approach on the following three SSL benchmark datasets.

CIFAR-10. CIFAR-10 dataset (Krizhevsky, 2009) contains colored images distributed across 10 classes. Those classes represent objects like airplanes, frogs, etc. It contains 50,000 training samples and 10,000 testing samples each of the size 32×32.

CIFAR-100. CIFAR-100 dataset (Krizhevsky, 2009) is similar to CIFAR-10 with the same number of training and testing samples, however, it contains 100 classes.

SNHN. SVHN dataset (Netzer et al., 2011) contains 73,257 training and 26,032 testing samples. The samples are colored images of the size 32×32, showing digits with various backgrounds.

For preprocessing, we normalize each sample so that it is in the range [0,1]. For the three datasets, we zero-pad each training sample with 2 pixels on each side. We then crop the resulting images randomly at the beginning of each epoch to obtain 32×32 training samples. On CIFAR-10 and CIFAR-100, we horizontally flip each sample with the probability of 0.5.

For validation, we reserve 5,000 training samples from each dataset. We train the models using a small randomly chosen set of labeled samples ($\mathcal{L}$) with replacement from the training set and the full training set as unlabeled set ($\mathcal{U}$) after discarding the corresponding labels. We report our results on the test set by averaging over three runs. For each dataset, we measure the performance using different sizes of the labeled set.

5.2 Settings

In order to emphasize the improvements driven by our method, we use ICT settings with only two minor changes which concern the preprocessing and the consistency regularization, see Sec. 3.2. More concretely, parameters that originate from ICT settings are learning rate, weight decay, N_{epoch}, N_{batch}, B, C_θ, $C_{\theta'}$, $w(t) \in [0, w_{\max}]$, β, and α. For the Cutmix operator, we use the parameters suggested in (Yun et al., 2019), see Sec. 3.2.

Relying on the exhaustive evaluations in (Cubuk et al., 2020), we define $\Omega_{\text{Aug}} = \{$autocontrast, equalize, posterize, rotate, solarize, shear-x/-y, translate-x/-y$\}$. For the magnitudes of the different augmentation transformations, we follow (Hendrycks* et al., 2020). Our implementation differs from RandAugment (Cubuk et al., 2020) in that we randomly sample M for each operation. For the hyperparameters of the ζ function and for τ, we conduct experiments on the validation sets in Sec. 5.1 and find that $d = 4$, $\varepsilon = 0.5$, and $\tau = 3/4 \cdot N_{\text{epoch}}$ perform well across all experiments.

We identify $\boldsymbol{\lambda_S}$, $\boldsymbol{\lambda_C}$, and $w_{\max}$ as hyperparameters to be adapted to the respective datasets. We conduct a search in $\{0, 1/3, 0.5\}$ for λ_S^i and λ_C^i under the conditions that $\sum_i \lambda_S^i = \sum_i \lambda_C^i = 1$. For $w_{\max}$, we search in $\{25, 50, 75, 100\}$ for CIFAR-10 and SVHN. For CIFAR-100, ICT does not provide any settings, so in the following, we present our settings. We notice that larger values for $w_{\max}$ seem to be required on CIFAR-100, so the search space becomes $\{1000, 1500, 2000\}$. Next, we give our final settings for the different datasets.

CIFAR-10. On CIFAR-10, for $L = 4000, 2000$, and 1000, we use $w_{\max} = 100$, $\lambda_S^1 = \lambda_S^2 = 0.5$, and $\lambda_C^1 = \lambda_C^2 = \lambda_C^3 = 1/3$.

CIFAR-100. On CIFAR-100, we use $N_{\text{epoch}} = 900$, where we use the CIFAR-10 setting from ICT for the first 600 training epochs followed by 300 epochs, where we ramp down the learning rate linearly to a final value of 0.0015. For $L = 10000$, we use $w_{\max} = 2000$, $\lambda_S^1 = \lambda_S^2 = 0.5$, and $\lambda_C^1 = \lambda_C^2 = \lambda_C^3 = 1/3$. For $L = 4000$, we use $w_{\max} = 1500$, $\lambda_S^1 = 1.0$, and $\lambda_C^1 = \lambda_C^2 = 0.5$.

SVHN. On SVHN, for $L = 1000$ and 500, we use $w_{\max} = 75$, $\lambda_S^1 = \lambda_S^2 = 0.5$, and $\lambda_C^1 = \lambda_C^2 = 0.5$. For $L = 250$, we use $w_{\max} = 25$, $\lambda_S^1 = 1.0$, and $\lambda_C^1 = \lambda_C^2 = 0.5$. In addition, following ICT, we use $\beta = 0.1$.

5.3 Results and Discussion

We report our results in terms of error rates averaged over three runs for SVHN and CIFAR-10 test sets in

Table 2: Error rates [%] on SVHN and CIFAR-10 test sets. We ran three trials for CGT. Note that † refers to methods using the WRN-28-2 architecture (Zagoruyko and Komodakis, 2016), while other methods use the CNN-13 architecture (Laine and Aila, 2016). Both architectures are comparable in terms of size and performance as also reported in ICT (Verma et al., 2019b).

	SVHN			CIFAR-10		
Method	$L=250$	$L=500$	$L=1000$	$L=1000$	$L=2000$	$L=4000$
Supervised (Verma et al., 2019b)	40.62 ± 0.95	22.93 ± 0.67	15.54 ± 0.61	39.95 ± 0.75	31.16 ± 0.66	21.75 ± 0.46
Supervised (Mixup) (Verma et al., 2019b)	33.73 ± 1.79	21.08 ± 0.61	13.70 ± 0.47	36.48 ± 0.15	26.24 ± 0.46	19.67 ± 0.16
MT (Tarvainen and Valpola, 2017)	4.35 ± 0.50	4.18 ± 0.27	3.95 ± 0.19	21.55 ± 1.48	15.73 ± 0.31	12.31 ± 0.28
TE+SNTG (Luo et al., 2018)	5.36 ± 0.57	4.46 ± 0.26	3.98 ± 0.21	18.41 ± 0.52	13.64 ± 0.32	10.93 ± 0.14
MUMR[2] (Ghorban et al., 2021)	-	-	4.67 ± 0.09	-	-	9.56 ± 0.23
DS (Ke et al., 2019)	-	-	-	14.17 ± 0.38	10.72 ± 0.19	8.89 ± 0.09
ICT (Verma et al., 2019b)	4.78 ± 0.68	4.23 ± 0.15	3.89 ± 0.04	15.48 ± 0.78	9.26 ± 0.09	7.29 ± 0.02
AdvMixup (Ma et al., 2020)	3.95 ± 0.70	3.37 ± 0.09	3.07 ± 0.18	9.67 ± 0.08	8.04 ± 0.12	7.13 ± 0.08
RealMix† (Nair et al., 2019)	3.53 ± 0.38	-	-	-	-	6.39 ± 0.27
MixMatch† (Berthelot et al., 2019)	3.78 ± 0.26	3.64 ± 0.46	3.27 ± 0.31	7.75 ± 0.32	7.03 ± 0.15	6.24 ± 0.06
Meta-Semi† (Wang et al., 2020)	-	4.12 ± 0.21	3.92 ± 0.11	7.34 ± 0.22	6.58 ± 0.07	6.10 ± 0.10
AFDA† (Mayer et al., 2021)	3.88 ± 0.13	-	3.39 ± 0.12	9.40 ± 0.32	-	6.05 ± 0.13
PLCB (Arazo et al., 2020)	3.66 ± 0.12	3.64 ± 0.04	3.55 ± 0.08	6.85 ± 0.15	-	5.97 ± 0.15
ReMixMatch† (Berthelot et al., 2020)	3.10 ± 0.50	-	2.83 ± 0.30	$\mathbf{5.73\pm0.16}$	-	5.14 ± 0.04
FeatMatch† (Kuo et al., 2020)	3.34 ± 0.19	-	3.10 ± 0.06	5.76 ± 0.07	-	4.91 ± 0.18
UDA† (Xie et al., 2020)	5.69 ± 2.76	-	2.46 ± 0.24	-	-	4.88 ± 0.18
FixMatch† (Sohn et al., 2020)	$\mathbf{2.64\pm0.64}$	-	$\mathbf{2.36\pm0.19}$	-	-	$\mathbf{4.31\pm0.15}$
CGT (ours)	2.93 ± 0.13	$\mathbf{2.71\pm0.07}$	2.65 ± 0.09	6.24 ± 0.27	$\mathbf{5.61\pm0.23}$	4.73 ± 0.09

Tab. 2 and for CIFAR-100 test set in Tab. 3.

Methods reported in Tab. 2 use either the CNN-13 (Laine and Aila, 2016) or the WRN-28-2 (Zagoruyko and Komodakis, 2016) architecture. Both architectures are comparable in terms of size and performance as also reported in ICT (Verma et al., 2019b). For our experiments, we use the CNN-13 architecture.

On all datasets, the test errors obtained by CGT are competitive with other state-of-the-art SSL methods.

On SVHN, we observe that CGT results in at least a five-fold reduction in the test error of the supervised learning algorithm (Verma et al., 2019b). On SVHN and CIFAR-10, CGT performs ~ 1 percent point (pp) better than ICT using only one-fourth of the maximum used labels, e.g., on CIFAR-10 using 1000 labels we achieve $6.24\pm0.27\%$ while ICT achieves $7.29\pm0.02\%$ using 4000 labels. This improvement is achieved through CGT's improved loss calculation and augmentation methods. Note that CGT's barebone, as described in Sec. 3.2 and Sec. 5.2, is ICT. This demonstrates that CGT uses, through the introduced modifications, the available labels more efficiently than ICT.

Table 3: Error rates [%] on CIFAR-100 test set. We ran three trials for CGT. All methods use the CNN-13 architecture (Laine and Aila, 2016).

	CIFAR-100	
Method	$L=4000$	$L=10000$
MT (Tarvainen and Valpola, 2017)	45.36 ± 0.49	36.08 ± 0.51
LP (Iscen et al., 2019)	43.73 ± 0.20	35.92 ± 0.47
WA (Athiwaratkun et al., 2018)	-	33.62 ± 0.54
PLCB (Arazo et al., 2020)	37.55 ± 1.09	32.15 ± 0.50
Meta-Semi (Wang et al., 2020)	37.61 ± 0.56	30.51 ± 0.32
FeatMatch (Kuo et al., 2020)	$\mathbf{31.06\pm0.41}$	26.83 ± 0.04
CGT (ours)	31.88 ± 0.62	$\mathbf{26.74\pm0.25}$

Table 4: Ablation study on CIFAR-10 using 4000 labeled data points. Error rates [%] are reported across three trials. $d=i$ refers to applying i randomly chosen augmentation transformations from Ω_{Aug} (see 5.2) sequentially on one of the input arguments of Mixup and/or Cutmix.

Aspect, CIFAR-10, $L=4000$							
Mixup	Cutmix	3-Mixup	$d=2$	$d=4$	ζ	$\theta \leftarrow \theta'$	Error rate [%]
✓	-	-	-	-	-	-	6.90 ± 0.16
-	✓	-	-	-	-	-	6.73 ± 0.20
✓	✓	-	-	-	-	-	6.23 ± 0.01
✓	✓	✓	-	-	-	-	6.02 ± 0.13
✓	✓	✓	✓	-	-	-	5.17 ± 0.01
✓	✓	✓	-	✓	-	-	5.20 ± 0.04
✓	✓	✓	-	-	✓	-	4.93 ± 0.11
✓	✓	✓	-	-	✓	✓	4.73 ± 0.09

We observe that CGT seems to be less sensitive to the size of the labeled set compared to our baseline ICT. A comparison to the recent methods presented in Tab. 2 reveals that our approach is able to achieve state-of-the-art performance on SVHN and CIFAR-10. FixMatch (Sohn et al., 2020) which scores slightly higher than our method requires above 1 million training steps to fully converge while our method requires only 200 thousand training steps. In addition, FixMatch and UDA (Xie et al., 2020) utilize 7 times more unlabeled than labeled data in each step, which further increases the training time.

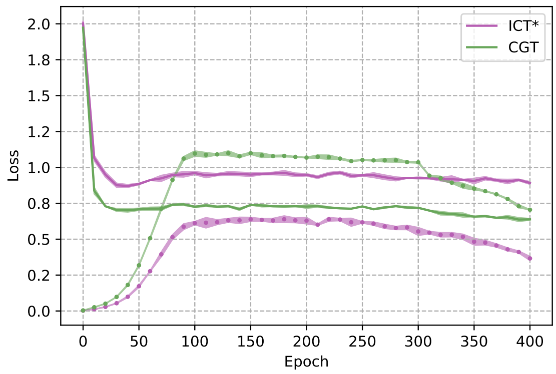

Figure 3: A comparison of the evolutions of the supervised (solid) and consistency (dotted) losses recorded over the training epochs for our baseline, ICT*, and CGT on CIFAR-10 using $L = 4000$.

Table 3 compares our results to recent methods on CIFAR-100. Here we compare only to methods that use the CNN-13 (Laine and Aila, 2016) architecture. Also here, we observe a competitive performance of our approach when compared to recent methods. Note that FixMatch (Sohn et al., 2020) is not included since it reports results on CIFAR-100 using WRN-28-8 which is much larger and thus not comparable to the above-mentioned architectures.

As described in Sec. 4, our approach in composed of multiple components. In Tab. 4, we show the contribution of each component by decomposing our method and conducting an ablation study. We observe that applying augmentation transformations, especially through the function composite ζ has a significant contribution to the final performance gain.

In order to determine the improvement that comes with overwriting θ with θ' during training, we stored each experiment from Tabs. 2 and 3 at its corresponding epoch τ and continued training without overwriting θ. The achieved error rates are shown in Tab. 5. Overwriting θ comes at virtually no additional computational cost and improves the performances across all the above experiments.

The supervised contribution to the loss function strives to minimize the entropy of predictions while the consistency contribution can practically lead to a trivial solution which corresponds to a maximized entropy, i.e., a zero consistency loss with θ^* for which $C_{\theta^*}(x_i) = (1/K, \ldots, 1/K)$ for any x_i. Considering the loss composition, the question arises: How should the consistency contribution behave in comparison to the supervised one for obtaining an optimal solution θ? Although we do not explicitly seek to answer this question, we show in the following a related observation that we assume to be relevant for further investigation. In ICT, we notice that the supervised contribution largely guides the training, i.e., it remains higher than the consistency contribution. CGT, however, has a lower supervised contribution and a significantly higher consistency contribution. Furthermore, the consistency contribution in CGT exceeds its supervised one, see Fig. 3, seemingly without having any negative effect on the performance.

Table 5: The effect of periodically overwriting θ with θ' starting from epoch τ.

SVHN		CIFAR-10		CIFAR-100	
$L = 250$	$L = 1000$	$L = 1000$	$L = 4000$	$L = 4000$	$L = 10000$
2.99 ± 0.10	2.69 ± 0.10	6.43 ± 0.28	4.93 ± 0.11	32.31 ± 0.54	27.25 ± 0.20

6 CONCLUSION

In this work, we have presented a simple yet efficient SSL algorithm, Consistency Guided Training (CGT). The CGT framework unifies multiple existing image-based augmentation techniques, namely the Mixup and CutMix operations. In addition, it utilizes new augmented versions of these operators where augmentations are stochastically applied to one side of the inputs of the Mixup and CutMix operators. Moreover, CGT involves a new generalization of the Mixup operator on unlabeled samples to regularize a larger region of the input space. The supervised and consistency losses in our framework are expressed as linear combinations of multiple constituents, each corresponding to a different augmentation transformation. Furthermore, our CGT framework has demonstrated to be benefitting from heavy augmentations of the unlabeled training data which enabled it to achieve state-of-the-art performance on three challenging benchmark datasets.

REFERENCES

Abadi, M., Barham, P., Chen, J., Chen, Z., Davis, A., Dean, J., et al. (2016). Tensorflow: A system for large-scale machine learning. In *Symposium on Operating Systems Design and Implementation*.

Arazo, E., Ortego, D., Albert, P., O' Connor, N. E., and McGuinness, K. (2020). Pseudo-labeling and confirmation bias in deep semi-supervised learning. In *International Joint Conference on Neural Networks*.

Athiwaratkun, B., Finzi, M., Izmailov, P., and Wilson, A. G. (2018). Improving consistency-based semi-supervised learning with weight averaging. *arXiv preprint arXiv:1806.05594*.

Berthelot, D., Carlini, N., Cubuk, E. D., Kurakin, A., Sohn, K., Zhang, H., and Raffel, C. (2020). Remixmatch: Semi-supervised learning with distribution alignment and augmentation anchoring. In *International Conference on Learning Representations*.

Berthelot, D., Carlini, N., Goodfellow, I., Papernot, N., Oliver, A., and Raffel, C. A. (2019). Mixmatch: A holistic approach to semi-supervised learning. In *Advances in Neural Information Processing Systems*.

Cubuk, E. D., Zoph, B., Mane, D., Vasudevan, V., and Le, Q. V. (2018). Autoaugment: Learning augmentation policies from data. *arXiv preprint arXiv:1805.09501*.

Cubuk, E. D., Zoph, B., Shlens, J., and Le, Q. V. (2020). Randaugment: Practical automated data augmentation with a reduced search space. In *Proceedings of the IEEE/CVF Conference on Computer Vision and Pattern Recognition Workshops*.

DeVries, T. and Taylor, G. W. (2017). Improved regularization of convolutional neural networks with cutout. *arXiv preprint arXiv:1708.04552*.

Ghiasi, G., Lin, T.-Y., and Le, Q. V. (2018). Dropblock: a regularization method for convolutional networks. In *Proceedings of the International Conference on Neural Information Processing Systems*.

Ghorban, F., Hasan, N., Velten, J., and Kummert, A. (2021). Improving fm-gan through mixup manifold regularization. In *International Symposium on Circuits and Systems*.

Ghorban, F., Marín, J., Su, Y., Colombo, A., and Kummert, A. (2018). Aggregated channels network for real-time pedestrian detection. In *International Conference on Machine Vision*.

Goodfellow, I., Shlens, J., and Szegedy, C. (2015). Explaining and harnessing adversarial examples. In *International Conference on Learning Representations*.

Hendrycks*, D., Mu*, N., Cubuk, E. D., Zoph, B., Gilmer, J., and Lakshminarayanan, B. (2020). Augmix: A simple method to improve robustness and uncertainty under data shift. In *International Conference on Learning Representations*.

Ho, D., Liang, E., Chen, X., Stoica, I., and Abbeel, P. (2019). Population based augmentation: Efficient learning of augmentation policy schedules. In *International Conference on Machine Learning*.

Iscen, A., Tolias, G., Avrithis, Y., and Chum, O. (2019). Label propagation for deep semi-supervised learning. In *Proceedings of the IEEE Conference on Computer Vision and Pattern Recognition*.

Kamnitsas, K., Castro, D., Le Folgoc, L., Walker, I., Tanno, R., Rueckert, D., Glocker, B., Criminisi, A., and Nori, A. (2018). Semi-supervised learning via compact latent space clustering. In *International Conference on Machine Learning*.

Ke, Z., Wang, D., Yan, Q., Ren, J., and Lau, R. W. (2019). Dual student: Breaking the limits of the teacher in semi-supervised learning. In *Proceedings of the IEEE International Conference on Computer Vision*.

Krizhevsky, A. (2009). Learning multiple layers of features from tiny images. Technical report, Master's thesis, Department of Computer Science, University of Toronto.

Kuo, C.-W., Ma, C.-Y., Huang, J.-B., and Kira, Z. (2020). Featmatch: Feature-based augmentation for semi-supervised learning. In *European Conference on Computer Vision*.

Laine, S. and Aila, T. (2016). Temporal ensembling for semi-supervised learning. *arXiv preprint arXiv:1610.02242*.

Li, W., Wang, Z., Li, J., Polson, J., Speier, W., and Arnold, C. W. (2019). Semi-supervised learning based on generative adversarial network: a comparison between good gan and bad gan approach. In *CVPR Workshops*.

Lim, S., Kim, I., Kim, T., Kim, C., and Kim, S. (2019). Fast autoaugment. *arXiv preprint arXiv:1905.00397*.

Luo, Y., Zhu, J., Li, M., Ren, Y., and Zhang, B. (2018). Smooth neighbors on teacher graphs for semi-supervised learning. In *Proceedings of the IEEE Conference on Computer Vision and Pattern Recognition*.

Ma, Y., Mao, X., Chen, Y., and Li, Q. (2020). Mixing up real samples and adversarial samples for semi-supervised learning. In *International Joint Conference on Neural Networks*.

Mayer, C., Paul, M., and Timofte, R. (2021). Adversarial feature distribution alignment for semi-supervised learning. *Computer Vision and Image Understanding*.

Miyato, T., Maeda, S.-i., Koyama, M., and Ishii, S. (2018). Virtual adversarial training: a regularization method for supervised and semi-supervised learning. *IEEE Transactions on Pattern Analysis and Machine Intelligence*.

Nair, V., Alonso, J. F., and Beltramelli, T. (2019). Realmix: Towards realistic semi-supervised deep learning algorithms. *arXiv preprint arXiv:1912.08766*.

Netzer, Y., Wang, T., Coates, A., Bissacco, A., Wu, B., and Ng, A. (2011). Reading digits in natural images with unsupervised feature learning. In *Advances in Neural Information Processing Systems*.

Qiao, S., Shen, W., Zhang, Z., Wang, B., and Yuille, A. (2018). Deep co-training for semi-supervised image recognition. In *Proceedings of the European Conference on Computer Vision*.

Sohn, K., Berthelot, D., Li, C.-L., Zhang, Z., Carlini, N., Cubuk, E. D., Kurakin, A., Zhang, H., and Raffel, C. (2020). Fixmatch: Simplifying semi-supervised learning with consistency and confidence. *arXiv preprint arXiv:2001.07685*.

Tarvainen, A. and Valpola, H. (2017). Mean teachers are better role models: Weight-averaged consistency targets improve semi-supervised deep learning results. In *Advances in Neural Information Processing Systems*.

Tokozume, Y., Ushiku, Y., and Harada, T. (2018). Between-class learning for image classification. In *Proceedings of the IEEE Conference on Computer Vision and Pattern Recognition*.

Verma, V., Lamb, A., Beckham, C., Najafi, A., Mitliagkas, I., Lopez-Paz, D., and Bengio, Y. (2019a). Manifold mixup: Better representations by interpolating hidden states. In *International Conference on Machine Learning*.

Verma, V., Lamb, A., Kannala, J., Bengio, Y., and Lopez-Paz, D. (2019b). Interpolation consistency training for semi-supervised learning. In *Proceedings of the International Joint Conference on Artificial Intelligence*.

Wang, Y., Guo, J., Song, S., and Huang, G. (2020). Meta-semi: A meta-learning approach for semi-supervised learning. *arXiv preprint arXiv:2007.02394*.

Wu, S., Deng, G., Li, J., Li, R., Yu, Z., and Wong, H.-S. (2019). Enhancing triplegan for semi-supervised conditional instance synthesis and classification. In *Proceedings of the IEEE Conference on Computer Vision and Pattern Recognition*.

Xie, Q., Dai, Z., Hovy, E., Luong, T., and Le, Q. (2020). Unsupervised data augmentation for consistency training. *Advances in Neural Information Processing Systems*.

Xie, Q., Peng, M., Huang, J., Wang, B., and Wang, H. (2019). Discriminative regularization with conditional generative adversarial nets for semi-supervised learning. In *International Joint Conference on Neural Networks*.

Yun, S., Han, D., Oh, S. J., Chun, S., Choe, J., and Yoo, Y. (2019). Cutmix: Regularization strategy to train strong classifiers with localizable features. In *Proceedings of the IEEE/CVF International Conference on Computer Vision*.

Zagoruyko, S. and Komodakis, N. (2016). Wide residual networks. In *British Machine Vision Conference*.

Zhang, H., Cisse, M., Dauphin, Y. N., and Lopez-Paz, D. (2018). mixup: Beyond empirical risk minimization. In *International Conference on Learning Representations*.

Zhong, Z., Zheng, L., Kang, G., Li, S., and Yang, Y. (2020). Random erasing data augmentation. In *Proceedings of the AAAI Conference on Artificial Intelligence*.